A new route to relativistic insulators: Lifshitz transition driven by spin fluctuations and spin-orbit renormalization in $NaOsO_3$

Bongjae Kim,[1] Peitao Liu,[1] Zeynep Ergönenc,[1] Alessandro Toschi,[2] Sergii Khmelevskyi,[1,3] and Cesare Franchini[1,*]

[1] *University of Vienna, Faculty of Physics and Center for Computational Materials Science, Vienna, Austria*
[2] *Institut für Festkörperphysik, Technische Universität Wien, Vienna, Austria*
[3] *Institute for Applied Physics, Technische Universität Wien, Vienna, Austria*

(Dated: December 23, 2016)

In systems where electrons form both dispersive bands and small local spins, we show that changes of the spin configuration can tune the bands through a Lifshitz transition, resulting in a continuous metal-insulator transition associated with a progressive change of the Fermi surface topology. In contrast to a Mott-Hubbard and Slater pictures, this spin-driven Lifshitz transition appears in systems with small electron-electron correlation and large hybridization. We show that this situation is realized in $5d$ distorted perovskites with an half-filled t_{2g} bands such as $NaOsO_3$, where the strong $p-d$ hybridization reduces the local moment, and spin-orbit coupling causes a large renormalization of the electronic mobility. This weakens the role of electronic correlations and drives the system towards an itinerant magnetic regime which enables spin-fluctuations.

PACS numbers: 71.30.+h, 75.47.Lx, 71.27.+a

arXiv:1601.03310v3 [cond-mat.str-el] 22 Dec 2016

Metal-to-insulator transitions (MITs) are one of the most important phenomena in solid-state physics and their fundamental understanding represents an enduring challenge in solid state theory [1, 2]. Different mechanisms have been invoked to explain the formation of an insulating regime. Classical examples are realized in $3d$ transition metal oxides (TMOs), where the nonconducting state is typically understood within the Mott-Hubbard model as arising from the competition between strong electron-electron interaction (U) and the electronic mobility, associated to the (non-interacting) bandwidth (W) [3–5]. When moving to the more spatially extended $4d$ and $5d$ orbitals the W increases and the U is expected to become smaller, leading to the tendency towards metallicity as in the itinerant magnet $SrRuO_3$ [6]. In contrast to these expectations, recent theory and experiment have revealed that in 'heavy' $5d$ TMOs, the enhanced spin-orbit coupling (SOC) strength [7] can lead to the formation of a variety of novel types of quantum states including unexpected insulating regimes [8–11]. In the most representative example, Sr_2IrO_4, the concerted action of a strong SOC and a moderate U leads to the opening of a small spectral gap [11, 12] denominated *relativistic Mott* gap. Other and more rare types of MITs have been recently proposed for magnetic relativistic osmium oxides based on the Slater mechanism [13–16], driven by antiferromagnetic (AFM) order, where the gap is opened by exchange interactions and not by electronic correlation, [17] or Lifshitz-like processes [18, 19], involving a rigid change of the Fermi surface topology [20].

In this work we show that in weakly correlated (small U) itinerant magnets the combined effect of longitudinal and rotational spin-fluctuations can cause a continuous MIT with Lifshitz characteristics, fundamentally different from relativistic Mott or purely Slater insulating states. The necessary conditions for the onset of this type of spin-driven Lifshitz MIT are the coexistence of a small U, a small local moment and an high degree of orbital hybridization. This places the system at the border of a magnetic and electronic instability where a Lifshitz MIT is possible. This situation can be realized in structurally-distorted, half-filled t_{2g}^3 (or close to half-filled) $5d$ oxides such as $NaOsO_3$ and $Cd_2Os_2O_7$ or iridates. By taking $NaOsO_3$ as a prototypical example, we show that here the balance between U and W is controlled by the SOC: the SOC induces a surprisingly large reduction of electronic mobility which renormalizes the U and pushes the system into a weakly correlated and magnetically itinerant regime subjected to spin fluctuations. We find that at high-temperature $NaOsO_3$ is a paramagnetic metal but as temperature decreases the changes of the amplitue and direction of the spins lead to the continuous vanishing of holes and electrons pockets in the Fermi surface (FS), that do not involve any substantial modification of the underlying band structure [20], consistent with a Lifshitz-type MIT.

Experimental observations indicate that $NaOsO_3$ undergoes a second-order MIT concomitant with the onset of an antiferromagnetic long-range ordering at a Néel temperature (T_N) of $\approx$ 410 K. This behavior is apparently adaptable to a Slater mechanism [13–16, 21]. However, the bad-metal behavior observed in a wide intermediate temperature region ($0.1T_N < T < T_N$) [13], the Curie-Weiss behavior of the susceptibility above T_N, and the need of a sizable U in Density Functional Theory (DFT) calculations to open the gap, is in conflict with an authentic Slater mechanism [21–23].

The fundamental properties of $NaOsO_3$ have been clearly exposed by Jung *et al.* [21]. In particular, it

* cesare.franchini@univie.ac.at

was shown that the apparent discrepancy between the measured Os ordered moment of only 1 μ_B[14] and the nominal t_{2g}^3 configuration should be attributable to the large $p-d$ hybridization that effectively reduces the local moment and form an (electronic and magnetic) itinerant background [21]. However, the authors concluded that the role of SOC is modest in this system, also based on the, reasonable, consideration that the t_{2g}^3 associated with a $L_{eff}=0$ state exhibits a negligible orbital moment, much smaller then the one of partially filled t_{2g} subshells [28, 29]. In the following we will show that relativistic effects can be strong even in a quenched orbital moment scenario, and we will explain that the SOC is the crucial effect in paving the way for the continuous MIT in $NaOsO_3$.

Spin-orbit induced renormalization. In the presence of a MIT in a TMO, the clarification of the role played by the electronic correlation U is a central aspect for the theoretical understanding. We begin, hence, by studying the effects of U and its interplay with the SOC for the case of our interest, $NaOsO_3$. All calculations were performed using the Vienna *ab initio* simulation package (VASP) [2] using the DFT+U method and including relativistic effects (see Supplement).

We start by computing the dependence of experimentally accessible observables on U. As usual, the value of the spectral gap Δ and the magnetic moment μ_{Os} are highly sensitive on the choice of U, as visualized in Figure 1(a). For $U=0$ the system is metallic, but for $U \geq 0.3$ eV $NaOsO_3$ exhibits a finite gap that increases linearly with U. The experimentally reported low-temperature optical gap, 0.1 eV [15] and the $\mu_{Os} \approx 1\ \mu_B$ [13] clearly indicate that the optimal value of U for $NaOsO_3$ should be chosen around 0.5 eV. At the same time, if we calculate U entirely *ab initio* within the constrained random phase approximation (cRPA) [27], neglecting all relativistic effects (SOC=0), we obtain $U^{noSOC}=1.58$ eV, a value similar to the one used in previous studies (i.e., $U=2$ eV [21–23]). As we demonstrate here, the root of this apparent controversy lays in the suprising "competition" between SOC and electronic correlation.

We study the interplay between SOC and correlation by comparing our DFT+U results with available infrared optical experiments. One rather general way[5, 30, 31] to estimate the degree of electronic correlation of a system is to evaluate the reduction of the electronic kinetic energy (mass renormalization) due to Coulomb repulsion. This can be quantified by the ratio K_{exp}/K_{DFT} between the experimentally measured kinetic energy (K_{exp}), determined by integrating over frequency the Drude contribution in the optical conductivity σ_D and the correpsonding "non-correlated" kinetic energy K_{DFT} obtained by DFT at $U=0$. Considering that σ_D can be expressed in terms of the plasma frequency, ω_p, via $\int d\omega\, \sigma_D(\omega) = \omega_p^2/8$, one

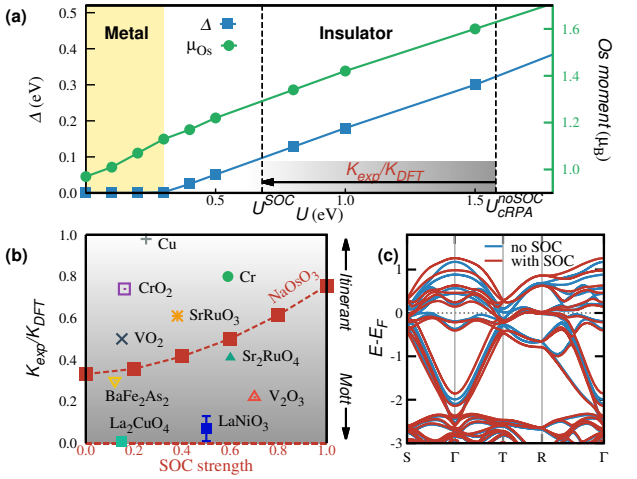

FIG. 1. (color online). Relativistic "renormalization" of the electronic correlation. (a) Energy gap and Os magnetic moment. (b) K_{exp}/K_{DFT} as a function of the SOC strength for $NaOsO_3$ and other reference systems. The measured data of the electron mobility are taken from Ref. [15] ($NaOsO_3$), Ref. [25] ($LaNiO_3$), and Ref. [5] (all other materials). (c) Paramagnetic band structure of $NaOsO_3$ with and without SOC.

can rewrite the kinetic energy ratio as:

$$\frac{K_{exp}}{K_{DFT}} = \frac{\omega_{p,exp}^2}{\omega_{p,DFT}^2} \qquad (1)$$

Surprisingly, K_{exp}/K_{DFT} in $NaOsO_3$ is dramatically dependent on the SOC strength as shown in Fig. 1(b). Without SOC, one should have classified the system as intermediate-strong correlated with $K_{exp}/K_{DFT}=0.33$, which is close to Fe-pnictide superconductors. As SOC is considered in the DFT calculations, however, K_{DFT} gets systematically reduced, as the estimated degree of correlation. For a full inclusion of SOC (SOC=1) we obtain K_{exp}/K_{DFT} =0.76, a value similar to those of conventional metals like Cr. To our best knowledge, $NaOsO_3$ represents the first system where such a strong renormalization of the balance between SOC and correlations is reported.

Supporting evidence for the importance of SOC in $NaOsO_3$ is provided by the computed SOC energy, 0.4 eV/Os, and by comparing the electronic structure with and without SOC (Fig. 1(b)). The inclusion of SOC leads to a widening of the band width by about 0.3 eV, a linearization of the band near Γ which yields the formation of a Dirac-like feature and, most importantly for the electron mobility, a band flattening near E_F that increases the effective masses and therefore decreases K_{DFT}.

Therefore, by turning on the SOC the estimated degree of correlation moves gradually from the border to the Mott-physics to the one of conventional metallic systems. This significant relativistic renormalization clarifies the origin of the abovementioned inconsistencies on the value

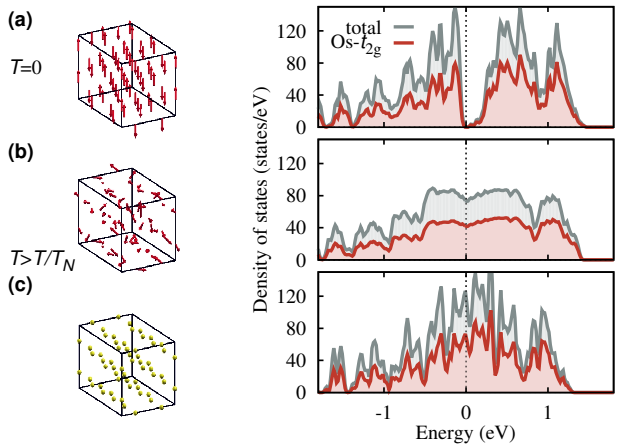

FIG. 2. (color online). High-temperature paramagnetic state. Total and t_{2g}-projected density of states (DOS) of the (a) low-temperature insulating AFM ground phase, (b) disordered paramagnetic phase (metallic) and (c) nonmagnetic phase (metallic). The arros indicate the Os sins.

of U in this system. More quantitatively, by rescaling the cRPA value of U^{noSOC} by the SOC-induced renormalization factor [31] we obtain $U^{SOC} = 0.68$ eV (comparable to the SOC energy) which leads to a much better description of the bandgap (see arrow in Fig. 1(a)). This smaller value of U is also consistent with the U proposed for similar compounds like $LiOsO_3$, $U < 1$ eV [32] and the itinerant magnet $SrRuO_3$, $U \approx 0.6$ eV [33].

Importantly, the analogy with $SrRuO_3$ is not limited to the low degree of correlation but also involves the magnetic itinerancy. Although $NaOsO_3$ exhibits a high T_N=410 K, the effective moment extracted from the the Curie-Weiss behavior of the high temperature susceptibility, 2.71 μ_B [13], is much higher than the ground state magnetic moment measured by neutron diffraction, ≈ 1 μ_B [14], indicating a large Rhodes-Wohlfarth ratio and suggestive of an itinerant antiferromagnetic behavior [34]. This magnetic itinerancy would *not* be compatible with a large U and is essential to explain the MIT in $NaOsO_3$, as discussed below.

Spin fluctuations and Lifshitz MIT. After clarifying the actual correlation degree in $NaOsO_3$ and the crucial role played by SOC to determine it, we are ready to address the most intriguing feature of this compound – the origin of the continuous MIT at finite temperatures.

Our main results are summarized in Figs. 2 and 3. First, we recall that the resistivity (ρ) curve of $NaOsO_3$ (Fig. 3(a)) shows two anomalies: one at $T_N = 410$ K, corresponding to a sudden increase of ρ, and the second one around T_A=30 K ($T/T_N \approx 0.1$) [13, 14] characterized by a steeper increment. The region below T_A has a clear insulating-like behavior with a large and rapidly growing ρ, whereas in the intermediate region, $T_A < T < T_N$, ρ is always smaller then 1 Ωcm and grows more slowly, with a bad-metal/pseudogap behavior. This hypothesis is supported by the experiments of Lo Vecchio *et al.* showing that the optical conductivity does neither vanish at T_N [15] nor shows a clear downturn at low frequencies in the intermediate temperature region. Such a peculiar temperature dependence of the conductivity is very unusual for TMOs [15], where -in the presence of a Mott-Hubbard MIT- the opposite trend can be observed [35].

Similar temperature dependence properties were reported, instead, for the narrow-gap semiconductor FeSi: at low temperature FeSi is a paramagnetic insulator but it develops a pseudogap associated with a bad-metal state as temperature increases [36–38]. This anomalous behavior is explained well by spin fluctuations in the context of the theory of itinerant magnetism elaborated by Moriya [39]. This similarity is of course very inspiring for the identification of the physical mechanisms at play in $NaOsO_3$.

To substantiate this idea we explore the effect of transverse (rotational) and longitudinal spin fluctuations by means of non-collinear fixed spin moment calculations. As a first step, we have simulated the effect of rotational spin fluctuations in the high-temperature spin disordered configuration by performing non-collinear magnetic calculations on large supercells containing 32 Os sites starting from randomly rotated Os spin moments in a paramagnetic arrangement (*i.e.*, the total magnetic moment is zero), by fixing the magnitude of the magnetic moments to the ground state value. The results are summarized in Fig. 2. The starting point is the density of states (DOS) of the reference collinear AFM insulating state at $T = 0$, Fig. 2(a). The paramagnetic DOS, Fig. 2(b), clearly shows that above T_N the system is an ordinary metal independently on the value of the local magnetic moment. By allowing a full relaxation of the moments the non-collinear paramagnetic state converges to a unrealistic metallic non-spin-polarized state (Fig. 2(c)) with entirely quenched local spin moments, similarly to the case of other magnetically itinerant metals like Cr and Ni [40]. However, longitudinal spin fluctuations induce local moments forming the true realistic high-temperature paramagnetic state [41]. Thus, to explain the double anomalies behavior in the resistivity curve at finite temperature (Fig. 3(a)), the effect of both rotational and longitudinal spin fluctuations should be taken into the account. To quantify the amplitude of the moments induced by longitudinal spin fluctuations at finite temperature we employ the phenomenological theory of Moriya, as described below [39].

Within spin-fluctuation theory there is a universal relation between the magnitude of the local mean square fluctuating magnetic moment at the transition temperature ($M = \sqrt{< M^2(T_N) >}$) and the ground state local moment (M_0) expressed by the Moriya formula $< M^2(T_N) >= 3/5 M_0^2$ [34, 39]. By combining the Moriya formula with the Mohn and Wohlfarth approximation [34], which assumes a linear temperature depen-

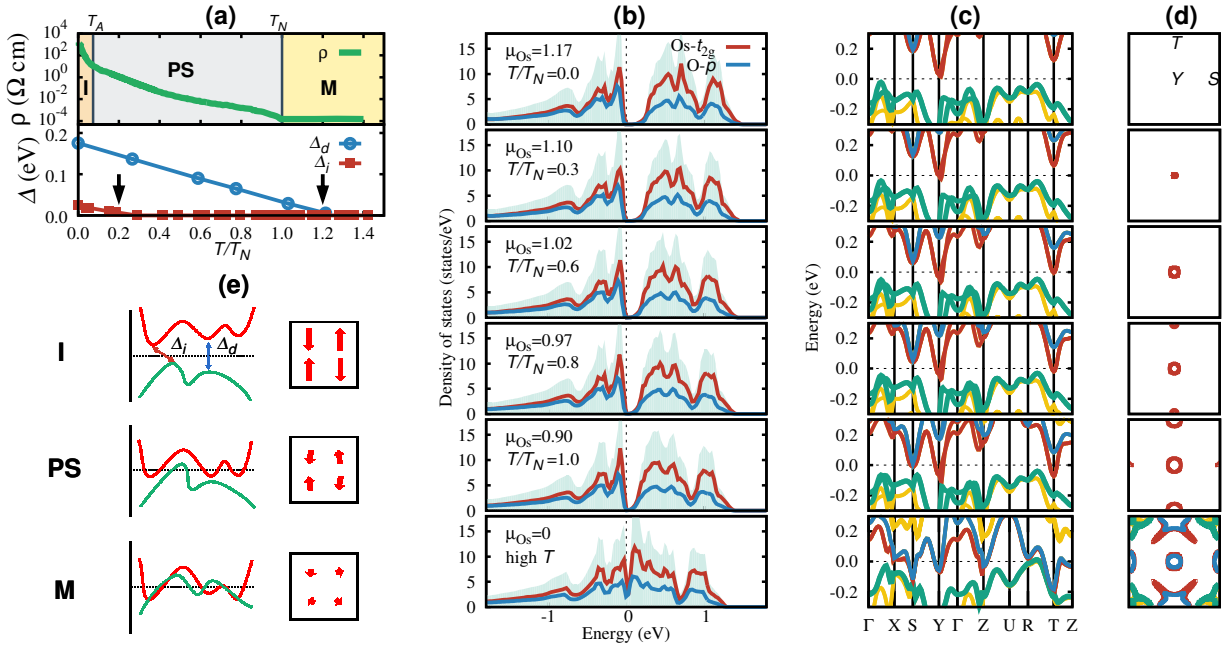

FIG. 3. (color online). Temperature-dependent MIT. (a) Indirect band gap (Δ_i) and direct pseudogap (Δ_d) as a function of temperature compared with the experimental resistivity curve readapted from Ref. [13]. The two anomalies in the resistivity curves at T_A and T_N set the transition from an insulating (I) to a pseudogap (PS) state and from the PS to a purely metal (M) state, respectively. These two anomalies are correlated with the closing of the insulating (Δ_i) and pseudo (Δ_d) gaps (indicated by arrows). (b) Partial DOS (c) band structure and (d) FS for different temperatures (T/T_N) corresponding to different Os magnetic moment μ_{Os} (Eq. 2). (e) Schematic diagram of the MIT. I: AFM insulator; PS: AFM pseudogap state with longitudinal (and small rotational) spin fluctuation; M: magnetically itinerant metal.

dence of the local mean square moment amplitude, we arrive to the following relation between the amplitude of the fluctuating Os moment ($M(T)$) and temperature:

$$M(T) = M_0\sqrt{1-\frac{2}{5}\frac{T}{T_N}}. \qquad (2)$$

Using this relation we have conducted a series of calculations with fixed magnetic moments from $\mu_{Os} = M_0 = 1.2\ \mu_B$ to 0 μ_B to examine the changes of the electronic structure upon temperature. The results are collected in Fig. 3. At $T = 0$ (top panels) the system is an antiferromagnetic insulator with a narrow bandgap and an Os moment μ_{Os}=1.17μ_B. As the temperature increases the resistivity curve shows its first anomaly at $T_A = T/T_N \approx 0.1$ (Fig. 3(a)), corresponding to the closing of the indirect band gap Δ_i due to longitudinal spin fluctuations that pushes down the conduction band minima at the Y point (Fig. 3(c)). Right above T_A, the system starts to develop a FS (Fig. 3(d)) and enters a bad-metal state characterized by several hole and electron pockets with a pseudogap (PS, see Fig. 3(e)) separating the valence and conduction bands. This pseudogap (Δ_d) decreases with temperature and finally closes for $M(T) = \mu_{Os} = 0.9\mu_B$ at about $T \simeq T_N$, second anomaly in the resistivity curve indicated by an arrow in Fig. 3(a). This second anomaly, due to the rotational magnetic disorder described previously, set the transition to a metallic behavior for $T > T_N$. The entire process is sketched schematically in Fig. 3(e).

By refining our analyis, and considering the corresponding evolution of the electronic bandstructure (Fig. 3(c)), we finally gain the complete description of the MIT in $NaOsO_3$. The bands changes almost rigidly with temperature and lead to a continuous change of the FS topology in terms of the appearance of progressively larger holes and electrons pockets (Fig. 3(d)): this represents a clear hallmark of a Lifshitz transition [19, 20].

Lifshitz transitions like the one described here are likely to be relevant for other magnetic materials laying at the border between a localized Mott picture and a metallic regime such as NiS [44], or 5d TMOs with a close to half-filled t_{2g}^3 configuration like $Cd_2Os_2O_7$ [18, 19] and iridates. Nearly half-filling, in fact, appears to be the optimum balance between a localized (insulating) and deloclaized (metallic) scenario: a reduced filling is generally associated to strong U picture [43] (i.e. d^1 Ba_2NaOsO_6 and d^2 Ba_2CaOsO_6 are Mott-like insulator [28]), whereas larger occupation increases the degree of metallicity (i.e. d^4 $BaOsO_3$ and $NaIrO_3$ [42]); moreover, the nearly $L_{eff} = 0$ state reduces the SOC-induced splitting which weaken the tendency towards Mott-SOC states and is functional for a rigid-band Lifshitz MIT. Also, structural distortions in 5d oxides are an impor-

tant factor for Lifshitz MIT as they enables the formation of small local moments that would be otherwise suppressed in undistorted and more strongly hybridized structures [21, 42].

Conclusions. In summary, we have shown that the coexistence between weak electronic correlation and itinerant magnetism can lead to a spin-driven Lifshitz MIT, *i.e.*, a magnetically induced continuous reconstruction of the Fermi surface. For $NaOsO_3$ we found that the MIT is prompted by transverse and longitudinal fluctuations of the itinerant Os moments, and is intimately bound to the SOC-driven renormalization of the electronic kinetic energy. Our study explains the three different regimes observed experimentally: (i) At low-T $NaOsO_3$ is an AFM insulator; (ii) At $T = T_A$ it enters a bad metal regime due to longitudinal spin fluctuations; finally (iii) at $T = T_N$ rotational spin fluctuations closes the direct pseudogap and the system become a paramagnetic metal. Spin fluctuations and the tunability by doping and pressure of the Lifshitz FS reconstruction could give rise to novel magnetic, orbital and superconducting transitions, to be exploited for engeneering TMOs based heterostructures. Moreover, the surprising role played by the SOC in $NaOsO_3$, as well as its "competitive" action against correlations -highlighted here for the first time- could radically affect the theoretical description of the relativistic mechanisms controlling the electronic properties of many other oxides.

[1] N. F. Mott, Metal-Insulator Transition. *Rev. Mod. Phys.* **40**, 677 (1968).

[2] M. Imada, A. Fujimori and Y. Tokura, Metal-insulator transitions, Rev. Mod. Phys. **70,** 1039 (1998).

[3] E. Dagotto, Complexity in Strongly Correlated Electronic Systems, Science **309,** 257 (2005).

[4] Y. Tokura and N. Nagaosa, Orbital Physics in Transition-Metal Oxides, Science **288,** 462 (2000).

[5] G. Kotliar and D. Vollhardt, Strongly Correlated Materials: Insights from Dynamical Mean-Field Theory, Physics Today **57**, 53 (2004).

[6] G. Koster, L. Klein, W. Siemons, G. Rijnders, J. S. Dodge, C.-B. Eom, D. H. A. Blank, and M. R. Beasley, Structure, physical properties, and applications of $SrRuO_3$ thin films, Rev. Mod. Phys. **84** 253 (2012)

[7] G. Cao, J. Bolivar, S. McCall, J. S. Crow, and R. P. Guertin, Weak ferromagnetism, metal-to-nonmetal transition, and negative differential resistivity in single-crystal Sr_2IrO_4, Phys. Rev. B **57,** R11039(R) (1998).

[8] Y. K. Kim, N. H. Sung, J. D. Denlinger, and B. J. Kim, Observation of a *d*-wave gap in electron-doped Sr_2IrO_4, Nature Physics **12**, 37 (2016).

[9] G. Jackeli and G. Khaliullin, Mott Insulators in the Strong Spin-Orbit Coupling Limit: From Heisenberg to a Quantum Compass and Kitaev Models, Phys. Rev. Lett. **102**, 017205 (2009).

[10] D. Pesin and L. Balents, Mott physics and band topology in materials with strong spin-orbit interaction, Nature Physics **6**, 376 (2010).

[11] B. J. Kim *et al.*, Novel $J_{eff} = 1/2$ Mott State Induced by Relativistic Spin-Orbit Coupling in Sr_2IrO_4, Phys. Rev. Lett. **101,** 076402 (2008).

[12] C. Martins, M. Aichhorn, L. Vaugier, and Silke Biermann, Reduced effective spin-orbital degeneracy and spin-orbital ordering in paramagnetic transition-metal oxides: Sr_2IrO_4 versus Sr_2RhO_4, Phys. Rev. Lett. **107**, 266404 (2011).

[13] Y. G. Shi *et al.*, Continuous metal-insulator transition of the antiferromagnetic perovskite $NaOsO_3$, Phys. Rev. B **80,** 161104(R) (2009).

[14] S. Calder *et al.*, Magnetically driven metal-insulator transition in $NaOsO_3$, Phys. Rev. Lett. **108,** 257209 (2012).

[15] I. Lo Vecchio, A. Perucchi, P. Di Pietro, O. Limaj, U. Schade, Y. Sun, M. Arai, K. Yamaura, and S. Lupi, Infrared evidence of a Slater metal-insulator transition in $NaOsO_3$, Sci. Rep. **3**, 2990 (2013).

[16] S. Calder *et el.*, , Enhanced spin-phonon-electronic coupling in a 5d oxide, Nat. Commun. **6**, 8916 (2015).

[17] J. C. Slater, Magnetic Effects and the Hartree-Fock Equation, Phys. Rev. **82**, 538 (1951).

[18] Hiroshi Shinaoka, Takashi Miyake, and Shoji Ishibashi, Noncollinear magnetism and spin-orbit coupling in 5d pyrochlore oxide $Cd_2Os_2O_7$, Hiroshi Shinaoka, Takashi Miyake, and Shoji Ishibashi Phys. Rev. Lett. **108**, 247204(1-4) (2012); Z. Hiroi, J. Yamaura, T. Hirose, I. Nagashima, and Y. Okamoto, Lifshitz Metal-insulator transition induced by the all-in/all-out magnetic order in the pyrochlore oxide $Cd_2Os_2O_7$, APL Materials **3,** 041501 (2015).

[19] C. H. Sohn *et al.*, Optical spectroscopic studies of the metal-insulator transition driven by all-in-all-out. magnetic ordering in 5d Pyrochlore, Phys. Rev. Lett. **115**, 266402 (2015).

[20] I. M. Lifshitz, Anomalies of electron characteristics of a metal in the high pressure region, Sov. Phys. JETP **11,** 1130 (1960).

[21] M. C. Jung, Y. J. Song, K. W. Lee, and W. E. Pickett, Structural and correlation effects in the itinerant insulating antiferromagnetic perovskite $NaOsO_3$, Phys. Rev. B **87**, 115119 (2013).

[22] S. Middey, Saikat Debnath, Priya Mahadevan, and D. D. Sarma, $NaOsO_3$: A high Neel temperature 5d oxide, Phys. Rev. B **89**, 134416 (2014).

[23] Y. Du, X. Wan, L. Sheng, J. Dong, and S. Savrasov, Electronic structure and magnetic properties of $NaOsO_3$, Phys. Rev. B **85,** 174424 (2012).

[24] G. Kresse and J. Furthmüller, Efficient iterative schemes for *ab initio* total-energy calculations using a plane-wave basis set, Phys. Rev. B **54,** 11169 (1996).

[25] M. K. Stewart *et al.* , Optical study of strained ultrathin films of strongly correlated $LaNiO_3$, Phys. Rev. B **83** 075125 (2011).

[26] M. M. Qazilbash, J. J. Hamlin, R. E. Baumbach, L. Zhang, D. J. Singh, M. B. Maple, and D. N. Basov, Electronic correlations in the iron pnictides, Nat. Phys. **5,** 647650 (2009).

[27] F. Aryasetiawan, M. Imada, A. Georges, G. Kotliar, S. Biermann and A. I. Lichtenstein, Frequency-dependent local interactions and low-energy effective models from electronic structure calculations, Phys. Rev. B **70,** 195104 (2004).

[28] Shruba Gangopadhyay and Warren E. Pickett, Interplay between Spin-Orbit Coupling and Strong Correlation Effects: Comparison of Three Osmate Double Perovskites: Ba_2AOsO_6 (A=Na, Ca, Y), Phys. Rev. B **93**, 155126 (2016).
[29] P. Liu, S. Khmelevskyi, B. Kim, M. Marsman, D. Li, X.-Q. Chen, D. D. Sarma, G. Kresse and C. Franchini, Anisotropic magnetic couplings and structure-driven canted to collinear transitions in Sr_2IrO_4 by magnetically constrained noncollinear DFT, Phys. Rev. B **92**, 054428 (2015).
[30] A. J. Millis, A. Zimmers, R. P. S. M. Lobo, N. Bontemps and C. C. Homes, Mott physics and the optical conductivity of electron-doped cuprates, Phys. Rev. B **72**, 224517 (2005).
[31] Q. Si, Iron pnictide superconductors: Electrons on the verge, Nat. Phys. **5,** 5 (2009).
[32] G. Giovannetti and M. Capone, Dual nature of the ferroelectric and metallic state in $LiOsO_3$, Phys. Rev. B **90,** 195113 (2014).
[33] J. M. Rondinelli, N. M. Caffrey, S. Sanvito, and N. A. Spaldin, Electronic properties of bulk and thin film $SrRuO_3$: Search for the metal-insulator transition, Phys. Rev. B **78,** 155107 (2008).
[34] P. Mohn, *Magnetism in the Solid State.* (Springer, 2006).
[35] L. Baldassarre *et al.*, S. Quasiparticle evolution and pseudogap formation in V_2O_3: An infrared spectroscopy study Phys. Rev. B **77**, 113107 (2008).
[36] A. Damascelli, K. Schulte, D. van der Marel, M. Fäth, A. A. Menovsky, Optical phonons in the reflectivity spectrum of FeSi, Physica B **230,** 787 (1997).
[37] S. Paschen, E. Felder, M. A. Chernikov, L. Degiorgi, H. Schwer, H. R. Ott, D. P. Young, J. L. Sarrao, and Z. Fisk, Low-temperature transport, thermodynamic, and optical properties of FeSi, Phys. Rev. B **56,** 12916 (1997).
[38] V. V. Mazurenko, A. O. Shorikov, A. V. Lukoyanov, K. Kharlov, E. Gorelov, A. I. Lichtenstein and V. I. Anisimov, Metal-insulator transitions and magnetism in correlated band insulators: FeSi and $Fe_{1-x}Co_xSi$, Phys. Rev. B **81,** 125131 (2010).
[39] T. Moriya, *Spin Fluctuations in Itinerant Electron Magnetism* (Springer Series in Solid-State Sciences, 1985).
[40] J. Kübler, *Theory of Itinerant Electron Magnetism* (Oxford Science Publications, 2000).
[41] S. Khmelevskyi, First-principles modeling of longitudinal spin fluctuations in itinerant electron antiferromagnets: High Néel temperature in the V3Al alloy Phys. Rev. B **94**, 024420 (2016).
[42] Myung-Chul Jung and Kwan-Woo Lee, Electronic structures, magnetism, and phonon spectra in the metallic cubic perovskite $BaOsO_3$, Phys. Rev. B **90**, 045120 (2014).
[43] Peitao Liu, Michele Reticcioli, Bongjae Kim, Alessandra Continenza, Georg Kresse, D.D. Sarma, Xing-Qiu Chen, Cesare Franchini, arXiv:1606.09112 [cond-mat.str-el].
[44] S. K. Panda, I. Dasgupta, E. Şaşioğlu, S. Blügel, and D. D. Sarma, NiS - An unusual self-doped, nearly compensated antiferromagnetic metal, Sci. Rep. **3**, 2995 (2013).

ACKNOWLEDGEMENTS

We thank A. Perucchi, S. Lupi and L. Boeri for helpful discussions. This work was supported by the joint FWF and Indian Department of Science and Technology (DST) project INDOX (I1490-N19), and by the FWF-SFB ViCoM (Grant No. F41). Computing time at the Vienna Scientific Cluster is greatly acknowledged.

Supplementary information: A new route to relativistic insulators: Lifshitz transition driven by spin fluctuations and spin-orbit renormalization in $NaOsO_3$

COMPUTATIONAL DETAILS

All calculations were performed using the Vienna *ab initio* simulation package (VASP) [S1, S2] using the DFT+U method [S3] within the generalized gradient approximation and including spin-orbit interaction (with quantization axis along the (0, 0, 1) direction). The on-site Coulomb U was computed fully *ab initio* using the constrained random phase approximation (cRPA) [S4]. For the cRPA calculations we used a maximally-localized Wannier functions basis including the t_{2g} states that ensured an excellent match with the DFT band structure around the Fermi energy as shown in Fig. S1). We used U = 0.4 eV, slightly smaller than the value estimated by the cRPA, 0.68 eV (see main text). We adopted the generalized gradient approximation, U=0.4 eV, plane-wave cutoff of 400 eV and a t_{2g} basis set for cRPA. The atomic position were fully relaxed at the experimental volume. A 10×6×10 Monkhorst-Pack mesh was used (4×3×4 and 20×20×20 for non-collinear calculations and plasma frequency calculations, respectively). The lattice parameters were fixed to the experimental ones and internal positions of all atoms were fully relaxed. A 10×6×10 Monkhorst-Pack mesh was used (reduced to 4×3×4 for non-collinear magnetic calculations in the large supercell containing 32 Os sites) with a plane-wave energy cutoff of 400 eV. In order to estimate the role of relativistic effects on the electron correlation (relativistic renormalization) we have followed the standard procedure described in Ref.S5 which involves the calculation of the plasma frequency in the paramagnetic phase using U = 0. For these calculations we increased the k-point grid up to 20×20×20 and very stringent energy convergence criteria (10^{-8} eV).

To model the high-temperature paramagnetic phase we adopted a supercell containing 32 Os sites starting from randomly distributed magnetic moments within a non-collinear set-up resulting in a zero total magnetic moment [S6–S8]. The degree of disorder was verified by computing the spin-spin correlation function S: for the random system we have obtain S=0.2, to be compared with the ordered AFM system for which S=1.

[S1] G. Kresse and J. Hafner, Ab initio molecular dynamics for liquid metals, Phys. Rev. B **47,** 558 (1993).

[S2] G. Kresse and J. Furthmüller, Efficient iterative schemes for *ab initio* total-energy calculations using a plane-wave basis set, Phys. Rev. B **54,** 11169 (1996).

[S3] S. L. Dudarev, G.A. Botton, S. Y. Savrasov, C. J. Humphreys, and A. P. Sutton, Electron-energy-loss spectra and the structural stability of nickel oxide: An LSDA+U study, Phys. Rev. B **57,** 1505 (1998).

[S4] F. Aryasetiawan, K. Karlsson, O. Jepsen, and U. Schönberger, Phys. Rev. B **74**, 125106 (2006).

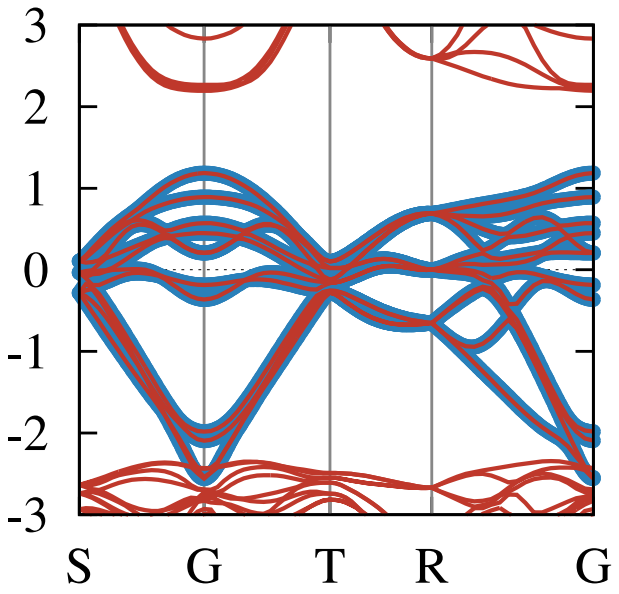

FIG. S1. Superimposition of the DFT and t_{2g} wannier-projected band structure.

[S5] M. M. Qazilbash, J. J. Hamlin, R. E. Baumbach, L. Zhang, D. J. Singh, M. B. Maple, and D. N. Basov, Electronic correlations in the iron pnictides, Nat. Phys. **5,** 647650 (2009).

[S6] S. V. Okatov, A. R. Kuznetsov, Yu. N. Gornostyrev, V. N. Urtsev, and M. I. Katsnelson, Effect of magnetic state on the γ-α transition in iron: First-principles calculations of the Bain transformation path, Phys. Rev. B **79**, 094111 (2009).

[S7] A.L. Wysocki, R.F. Sabirianov, M. van Schilfgaarde, K.D. Belashchenko, First-principles analysis of spin-disorder resistivity of Fe and Ni, Phys. Rev. B **80**, 224423 (2009).

[S8] J.K. Glasbrenner, K.D. Belashchenko, J. Kudrnovsky, V. Drchal, S. Khmelevskyi, I. Turek, First-principles study of spin-disorder resistivity of heavy rare-earth metals: Gd-Tm series. Phys. Rev. B **85**, 214405(2012).